J Porous Mater (2017) 24:1253–1261
DOI 10.1007/s10934-017-0366-5

Synthesis and catalytic properties of copper(II) Schiff-base complex immobilized silica materials

G. Anbarasu[1] · M. Malathy[1] · R. Rajavel[1]

Published online: 6 February 2017
© Springer Science+Business Media New York 2017

Abstract Cu(II) Schiff base complex immobilized silica was prepared via the one pot reaction of thiophene-2-carbaldehyde with silica functionalized 3-aminopropyltriethoxysilane (APTES) and copper acetate by refluxing in ethanol. The formation of this complex was confirmed by FT-IR, UV–DRS, XRD, SEM, EDX, ICP-AES and BET analytical methods. In addition, the catalytic activity of the as synthesized Cu(II) Schiff base complex immobilized silica was evaluated through the oxidative coupling of benzylamines to the corresponding imines. The catalyst was easily recovered and reused for five times without any significant loss of its catalytic activity.

Keywords Copper(II) Schiff-base complex · 2-Thiophenecarboxaldehyde · 3-Aminopropyltriethoxysilane · Oxidative coupling

1 Introduction

Imines are also known as Schiff bases and are versatile and valuable building blocks in organic synthesis. In an addition to that, they are useful intermediates in various organic reactions such as cyclization, reduction, addition, condensation and fine chemicals [1, 2] such as amides, chiral amines, oxazolidines, hydroxyamines, and nitrones [3]. Numerous methodologies have been developed to synthesize imines, including oxidation of primary [4] or secondary [5] amines, condensation of amines with aldehydes, and oxidative condensation of amines with alcohols [6]. In the recent year, considerable attention has been paid for the selective synthesis of imines from the oxidation of primary amines. Because, which prevent the formation of other undesired nitrogen-containing compounds [7]. There are numerous reports available in the literature for the synthesis of imines from the oxidation of primary amines using homogeneous methods [8], but only the few reports only available for the synthesis of imines using heterogeneous methods [9]. However, many of these synthetic methodologies were associated with some disadvantages like longer reaction times, expensive reagents, harsh conditions, and low product yields, occurrence of several side products and difficulty in recovery and reusability of the catalysts. So, we still need for an efficient, eco-friendlier method for the synthesis of imine from the oxidative coupling reactions of amines. Recently, immobilization transition metal complexes on to the silica material was received an active area of research in the field of organic synthesis, catalysis, adsorption, separation and sensing [10]. Because, silica functionalized material has some specific properties like, non-swelling properties, large specific surface area, fast kinetics, and high selectivity, good mechanical, thermal and chemical stability [11, 12].

From the brief background of this, we wish to report the synthesis of a novel thiophene-2-carbaldehyde based copper(II) Schiff-base complex immobilized silica material. The as synthesized copper(II) Schiff-base complex immobilized silica material was an efficient catalyst towards the self-oxidative coupling of benzylamines to the corresponding imines.

✉ R. Rajavel
drrajavelpu@gmail.com

[1] Department of Chemistry, Periyar University, Periyar Palkalai Nagar, Salem, Tamil Nadu 636 011, India

2 Experimental

2.1 Materials and instruments

3-Aminopropyltriethoxysilane (3-APTES) was purchased from Sigma Aldrich and all the other reagents and solvents were purchased from Loba Chemie. FT-IR spectra of the samples were recorded in the region of 4000–400 cm^{-1} on Shimadzu spectrophotometer using KBr pellet technique. Diffuse reflectance spectra were obtained on an UV–DRS Ocean Optics px-2 spectrometer with pulsed xenon light source. Powder X-ray diffraction (XRD) patterns were recorded on a Rigaku Mini Flex II diffractometer (Tokyo, JAPAN). The surface morphology of the synthesized material was analyzed by using scanning electron microscope (HRSEM, JSM 840A, JEOL-Japan) equipped with EDX. The Cu loading in the catalyst were determined using inductively coupled plasma atomic emission spectroscopy (ICP-AES) analysis on a Thermo Electron IRIS Intrepid II XSP DUO. BET Surface area was calculated by Brunauer Emmett and Teller Equation using multipoint adsorption in the P/P_0 range 0.05–0.33. Micro pore size distribution was calculated using Horvath–Kawazoe and BJH method.

2.2 Catalyst preparation

2.2.1 *Synthesis of APTES functionalized silica (SiO_2–APTES)*

The synthesis protocol for installing APTES on to SiO_2 was adapted from the earlier reported procedure [13]. Typically, 3 g Silica gel with particle size in the range of 60–120 mesh was treated with nitric acid (HNO_3:H_2O = 1:1) at 100 °C for 3 h, and then hydrochloric acid (6 mol l^{-1}) at 100 °C for 8 h. The treated silica gel was washed with doubly distilled water (DDW) and dried first at 120 °C for 24 h, and finally calcined in muffle furnace at 180 °C for 2 h. Then, 3 g pre-treated silica was taken in 100 ml of dichloromethane and 2.0 mmol of APTES was added and the resultant mixture was refluxed for 24 h. After cooling, the solids were separated by filtration and washed repeatedly with dichloromethane and dried under vacuum at 50 °C. The resulting material was then dried at 120 °C for 24 h and designated as SiO_2–APTES.

2.2.2 *Functionalization of [Cu(OAc)$_2$] onto (SiO_2–APTES) [Cu(II)@imine–SiO_2]*

To a suspension of 2.5 g of APTES@SiO_2 in 60 ml ethanol was added 2.12 mmol of 2-thiophenecarboxaldehyde in small portions. The reaction mixture was refluxed for 8 h completely to form Schiff Base ligand. Then copper(II) acetate 0.5 g in EtOH was added and refluxing was continued for another 8 h. While refluxing the color of the reaction mixture was slowly change from light yellow to green. After completion the reaction mixture was cooled at room temperature and the solid was filtered and washed with hot ethanol to remove the unreacted copper acetate and dried under vacuum. The green colored Silica material was designated as Cu(II)@imine–SiO_2. The outline for the preparation of this Cu(II) Schiff base immobilized Silica was shown in Scheme 1.

2.3 General experimental procedure for the oxidation of benzylamines to imines

A mixture of benzylamine (1 mmol) and catalyst (Cu(II)@imine–SiO_2) were taken in RB flask and the mixture was heated under solvent free condition at 100 °C until the completion of the reaction. After completion diethyl ether was added to the reaction mixture and the mixture was stirred for 10 min. Then, the catalyst was separated out by filtration and the filtrate was concentrated under reduced pressure. All the synthesized compounds are known compounds and their physical data were matched with those are reported in literature.

3 Results and discussion

3.1 Characterization of catalyst

The synthesized Cu(II) Schiff base complex immobilized silica was confirmed by IR, UV–DRS, XRD, SEM, EDX, ICP-AES and BET analysis.

3.1.1 *FT-IR spectroscopy*

The FTIR spectra of (a) activated SiO_2, (b) SiO_2–APTES, (c) SiO_2–APTES–imine, (d) Cu(II)@imine–SiO_2 were presented in Fig. 1. In activated silica, a broad stretching band appeared around 3446 cm^{-1} in the spectrum of due to the O-H stretching vibration of silanol group and adsorbed water. The intense band at 1093 cm^{-1} should be related to Si–O–Si stretching vibration. The peaks observed at around 804 and 451 cm^{-1} were attributed to the typical symmetric and bending vibrations of Si–O–Si group (Fig. 1a) [14]. All these characteristic peaks were also present in the FT-IR spectra of all the modified forms of SiO_2, which indicated that SiO_2 framework is not affected even after the chemical modifications.

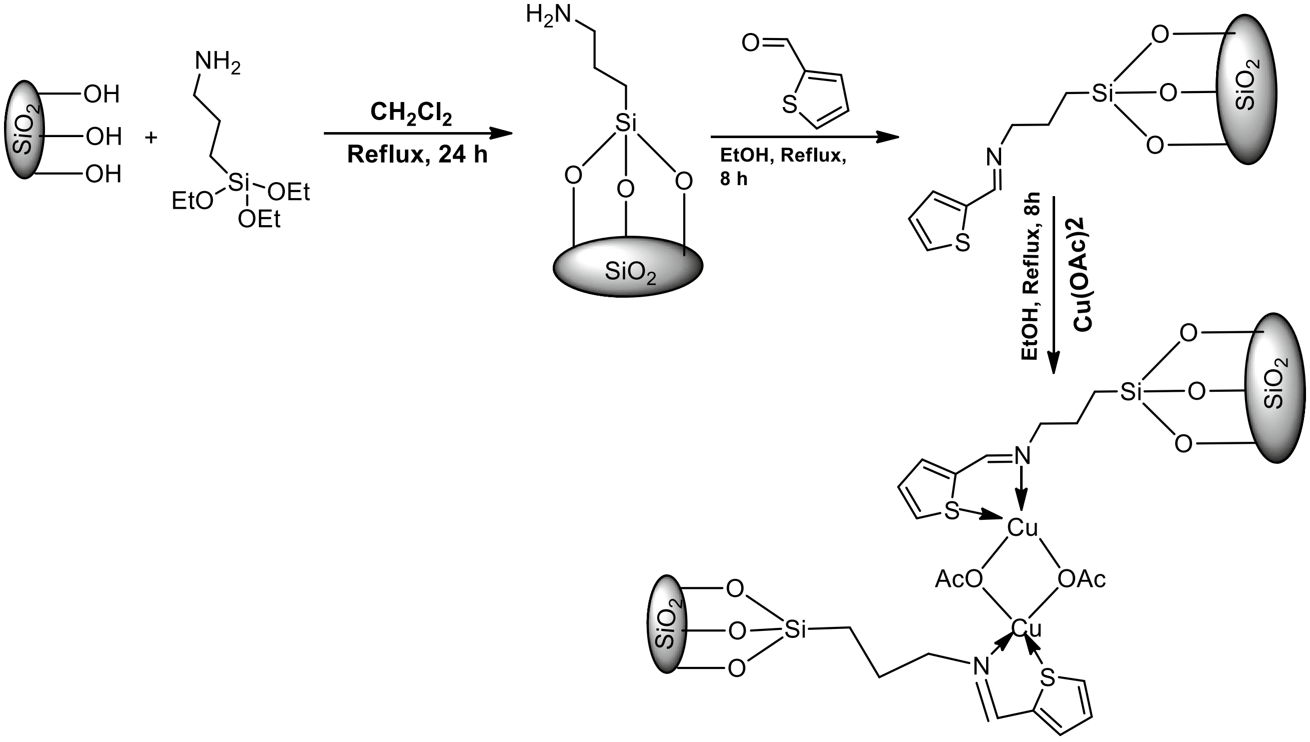

Scheme 1 Schematic representation for synthesis of copper(II) Schiff base complex immobilized silica (Cu(II)@imine–SiO_2)

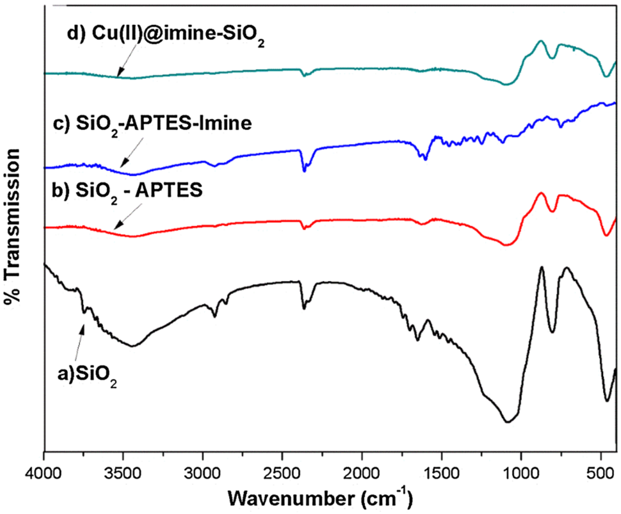

Fig. 1 IR spectra of *a* SiO_2, *b* SiO_2–APTES, *c* SiO_2–APTES–imine, *d* Cu(II)imine–SiO_2

But, in the case of SiO_2–APTES, a new band in the region of 3290–3000 cm^{-1} might be due to the –NH stretching vibration. In addition to that, the occurrence of stretching and bending vibrations of methylene groups observed at 2368 and 1495 cm^{-1} (Fig. 1b). The –OH stretching vibration was shifted to a lower wave number region, which confirms the grafting of APTES on to surface of silica. Whereas, in the case of SiO_2–APTES@imine, the –NH stretching vibration peak was disappeared and a new peak appeared at 1639 cm^{-1} corresponds to the –C=N stretching vibration (Fig. 1c). But, in Cu(II) Schiff base complex immobilized silica, the –C=N stretching vibration was shifted to lower wave number (1618 cm^{-1}) region indicating the –C=N bond was coordinated to copper through the lone pair electrons of nitrogen. The two strong bands at 1555 cm^{-1} [15] and 1436 cm^{-1} [16] could be assigned for the asymmetric and symmetric vibrations of the bridging acetate ions and a weak peak at 424 cm^{-1} was indicated the stretching vibration of Cu–N group (Fig. 1d) [12]. From this, we concluded that the formation of Cu(II) Schiff base complex immobilized silica.

3.1.2 *UV–vis DRS*

The UV–DR spectra of (a) activated SiO_2, (b) SiO_2–APTES–imine and (c) Cu(II)@imine–SiO_2 were illustrated in Fig. 2. The UV–DRS pattern of Si–APTES–imine showed a significant band at 318 nm which may be due to the characteristic π–π* transition –C=N in Schiff base ligand. In copper(II) Schiff base complex immobilized silica, the band was shifted to higher wavelength (324 nm) indicating that the ligand was

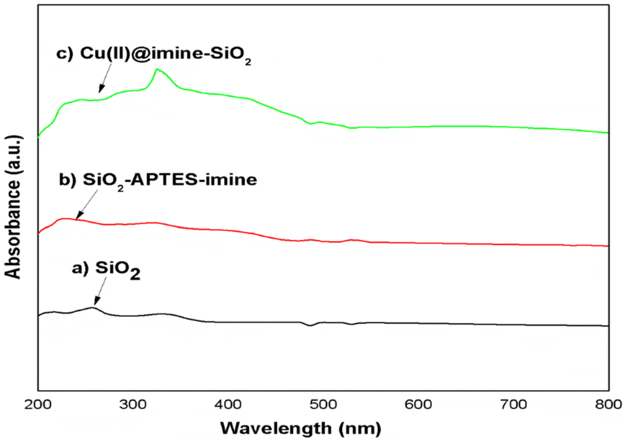

Fig. 2 UV–vis diffuse reflectance spectra of *a* SiO_2, *b* SiO_2–APTES–imine, *c* Cu(II)imine–SiO_2

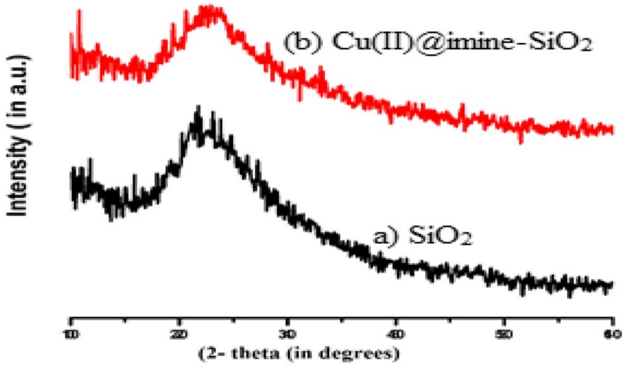

Fig. 3 XRD pattern of *a* SiO_2, *b* Cu(II)imine–SiO_2

coordinating to the copper complex. In addition, the electronic spectrum of the Cu(II) Schiff base complex immobilized silica exhibited two additional bands, one band at around 417 nm could be accounted for the charge transfer band between Cu^{2+} and the oxygen of the ligand [17, 18]. Another one broad absorption band in between 600 and 750 nm was due to the appearance of d–d transition.

3.1.3 Powder XRD

X-ray diffraction patterns of the activated silica and Cu(II) Schiff base complex immobilized silica were shown in Fig. 3. SiO_2 exhibited a broad band centered at $2\theta = 22°$ confers the amorphous nature and topological structure of the SiO_2 [19, 20]. On the other hand, Cu(II) Schiff base complex immobilized silica showed a low intensity peak at $2\theta = 21.17°$. This may be due to the slight disorder in the topological structure of SiO_2 in its modified forms because of the immobilization of Cu(II)@imine–SiO_2 and entry of metal ions on to the porous wall of SiO_2.

3.1.4 SEM–EDX

The surface morphology of SiO_2 and Cu(II)@imine–SiO_2 were shown in Fig. 4. The SEM image of the both activated SiO_2 and Cu(II)@imine–SiO_2 clearly showed the morphological change which occurred on the surface of silica before and after immobilized with Cu(II) Schiff base complex. From the Fig. 4, we have observed that both the activated silica as well as Cu(II) Schiff base complex immobilized silica were appeared as similar morphology with uniformed stone like structure. But, the particle size of Cu(II)@imine–SiO_2 was significantly decreased. The formation of this material was further confirmed by energy dispersive X-ray spectroscopy (EDS) (Fig. 4e). Also, to extend the scope of catalyst characterization, we have determined the exact loading of Cu(II) on silica by ICP-AES technique. The Cu(II) amount of the immobilized catalyst on SiO_2 was found to be 0.257 mmol g^{-1} or 50 mg.

3.1.5 N_2 adsorption–desorption isotherm

The N_2 adsorption and desorption isotherms of (a) SiO_2 and (b) Cu(II)@imine–SiO_2 are shown in Fig. 5 and the structural parameters are summarized in Table 1. This study provided the information about the specific surface area and porosity of the prepared samples. The isotherms of both the samples followed typical type IV patterns according to IUPAC classification with a typical hysteresis loop, featuring mesoporous material with highly uniform pore size distribution [21]. According to BET measurement, the surface area for SiO_2 was 387.8592 m^2/g which upon functionalized with Cu(II) Schiff base complex the surface area was decreased to 135.0752 m^2/g. Similarly, the pore volume of the material was also decreased (0.337398 cm^3/g) upon immobilized with Cu(II) Schiff base complex. But, the pore radius (2 V/A) of the synthesized Cu(II) Schiff base complex immobilized silica was increases (33.732 Å) than that of parent SiO_2 (18.578 Å). A considerable decrease in the BET surface area and pore volume of the Cu(II) Schiff base complex immobilized silica confirmed the organic moieties anchored successfully on the surface of SiO_2.

3.2 Catalytic activity

3.2.1 Oxidation of benzylamines to imines

The catalytic activity of the synthesized Cu(II) Schiff base complex immobilized silica material was evaluated by the

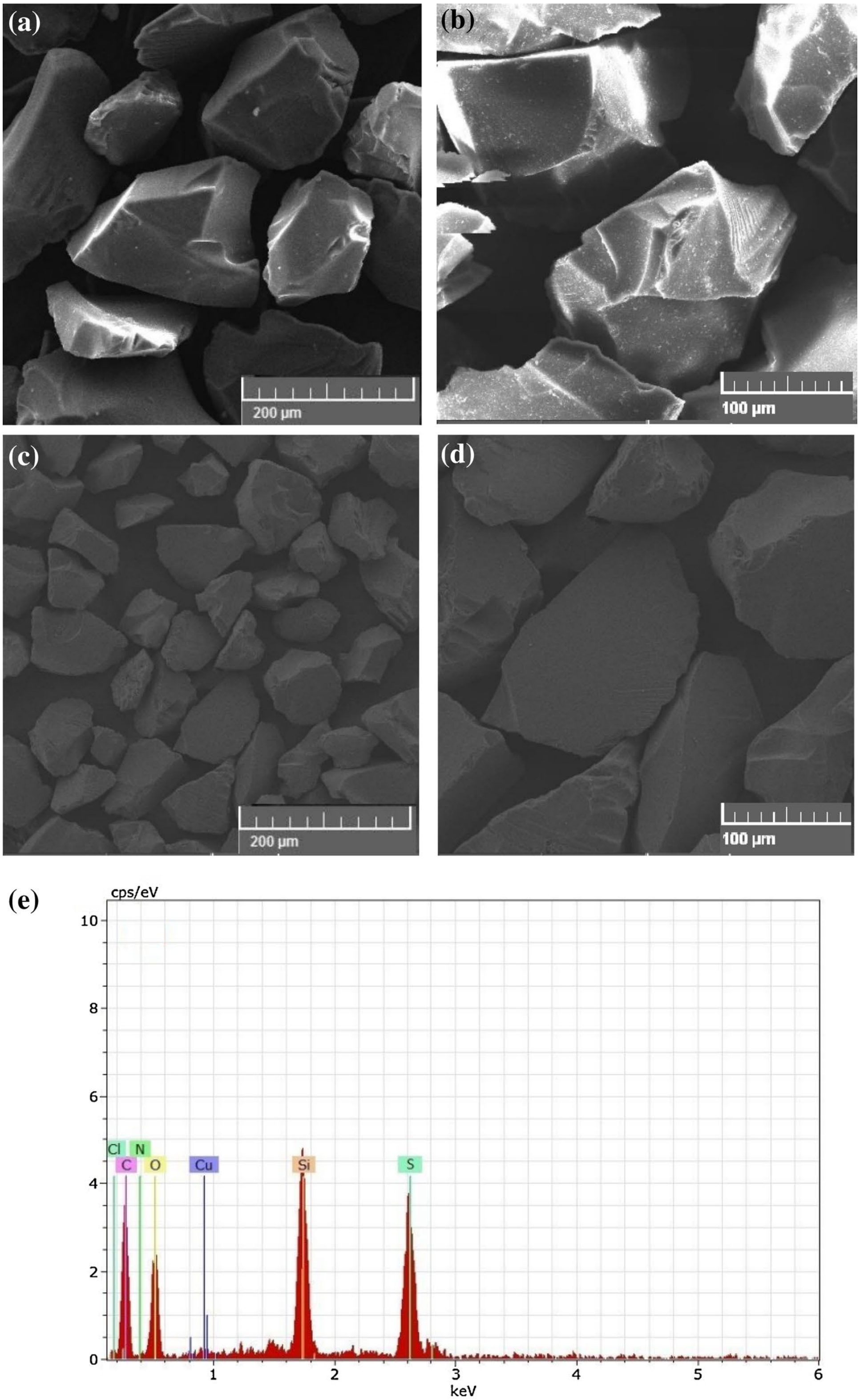

Fig. 4 Scanning electron micrographs of **a** and **b** activated SiO_2, **c** and **d** Cu(II)@imine–SiO_2 (*close-up view*), The *scale bar* represents 200 and 100 μm, **e** EDX spectrum of Cu(II)@imine–SiO_2

oxidation reaction of amines to imines (Scheme 2). In this regard, we have to optimize some reaction parameters such as, solvent, catalyst quantity, and temperature.

In order to study the suitability of solvents for this reaction, we have systematically carried out a model oxidation reaction of benzylamine by using 50 mg of Cu(II)@

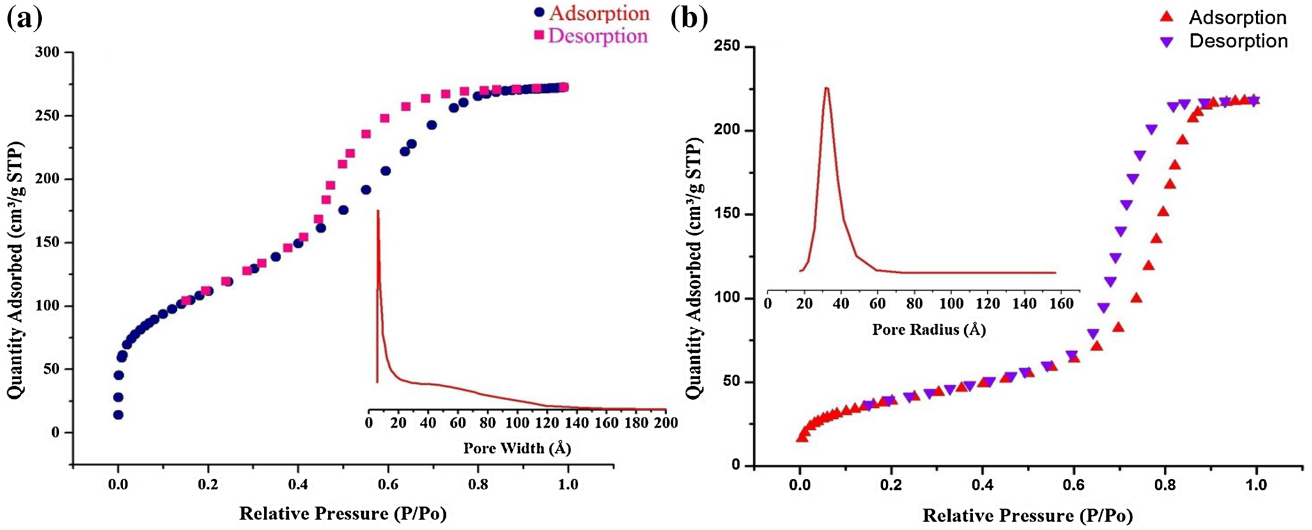

Fig. 5 N_2 Adsorption–Desorption isotherms and pore size distributions *inset* of **a** activated SiO_2 and **b** Cu(II)@imine–SiO_2

Table 1 Textural data on Surface area and pore size distribution of the silica based sample materials

Materials	Surface area (m^2/g)	Pore volume (cm^3/g)	Pore radius (2 V/A)
SiO_2	387.8592	0.421515	18.578 Å
Cu(II)@imine–SiO_2	135.0752	0.337398	33.732 Å

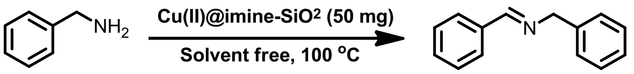

Scheme 2 Oxidative coupling reaction of benzylamines using Cu(II)@imine–SiO_2 as a catalyst

imine–SiO_2 as a catalyst with different solvents as well as under solvent free conditions and the results are presented in Table 2.

From this table, all the solvents are promoted this reaction and yielded the corresponding imines in moderate yields (Table 2, entries 1–7). But, in the case of chloro

Table 2 Optimization of reaction conditions

Entry	Solvent	Temperature (°C)	Reaction time (h)	Yield (%)[a]	TON[b]	TOF[c] (h^{-1})
1	Methanol	Reflux	9	67	260	30
2	Ethanol	Reflux	9	73	284	29
3	Isopropanol	Reflux	9	77	299	28
4	DMSO	100	9	45	175	33
5	DMF	100	9	40	155	17
6	THF	Reflux	9	65	252	28
7	Toluene	Reflux	9	71	276	31
8	Dichloromethane	Reflux	9	–	–	–
9	Chloroform	Reflux	9	–	–	–
10	Solvent free	100	2	98	381	191

Oxidative coupling reaction of benzylamines (1 mmol) using Cu(II)@imine–SiO_2 (50 mg, 0.257% Cu) as a catalyst in different solvents

[a] Isolated yield

[b] Turnover number (TON) = (mmol of product)/(mmol of catalyst) after time t

[c] TOF = TON/time

Table 3 Effect of catalyst amount and temperature

Entry	Catalyst amount (mg, mol%)	Temperature (°C)	Reaction time (h)	Yield (%)[a]	TON[b]	TOF[c] (h^{-1})
1	–	100	24	–	–	–
2	10, 0.051	100	18	37	725	40
3	20, 0.102	100	12	53	600	43
4	30, 0.154	100	7	65	422	60
5	40, 0.205	100	4	77	376	94
6	50, 0.257	100	2	98	381	191
7	100, 0.514	100	2	98	191	95
8	50, 0.257	RT	24	20	78	3
9	50, 0.257	50	10	57	221	22
10	50, 0.257	80	5	75	291	58
11	50, 0.257	120	2	98	381	191

Oxidative coupling reaction of benzylamines (1 mmol) using different quantity of Cu(II)@imine–SiO_2 (50 mg, 0.257% Cu) as a catalyst at different temperature under solvent free conditions

[a] Isolated yield

[b] Turnover number (TON) = (mmol of product)/(mmol of catalyst) after time t

[c] TOF = TON/time

Table 4 Substrate scope of the oxidative coupling reaction

Entry	Substrate	Product	Time (h)	Yield (%)[a]	TON[b]	TOF[c] (h^{-1})
1	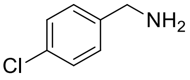	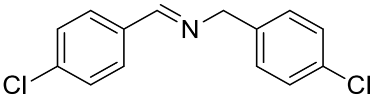	2	85	331	165
2	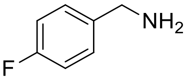	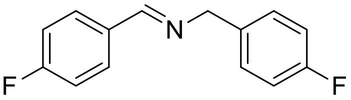	2	84	327	163
3	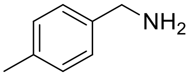	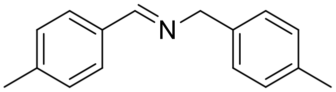	2	92	358	179
4	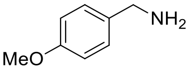	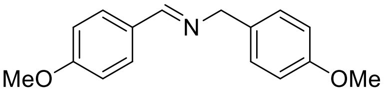	2	82	319	159
5	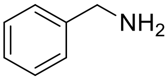	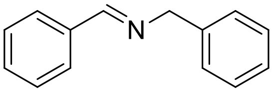	2	98	381	191

Oxidative coupling reaction of benzylamines (1 mmol) using (50 mg, 0.257% Cu) of Cu(II)@imine–SiO_2 as a catalyst under solvent free conditions at 100 °C

[a] Isolated yield

[b] Turnover number (TON) = (mmol of product)/(mmol of catalyst) after time t

[c] TOF = TON/time

solvents like dichloromethane and chloroform where the consistent product was not formed even after 10 h (Table 2, entries 8 and 9). As in the solvent media, the reaction time was long. So, in order to improve the product yield and reduce the time, the same oxidation reaction was conducted under solvent free conditions at 100 °C. Where, the corresponding imine was formed with 98% of yield in shorter time (2 h, Table 2, entry 10).

Next, we have studied the optimum quantity of Cu(II)@imine–SiO_2 needed for this transformation. Initially, this reaction was stated under catalyst free conditions, where the corresponding product was not formed even after 24 h

Scheme 3 Proposed mechanism for the oxidative coupling reaction

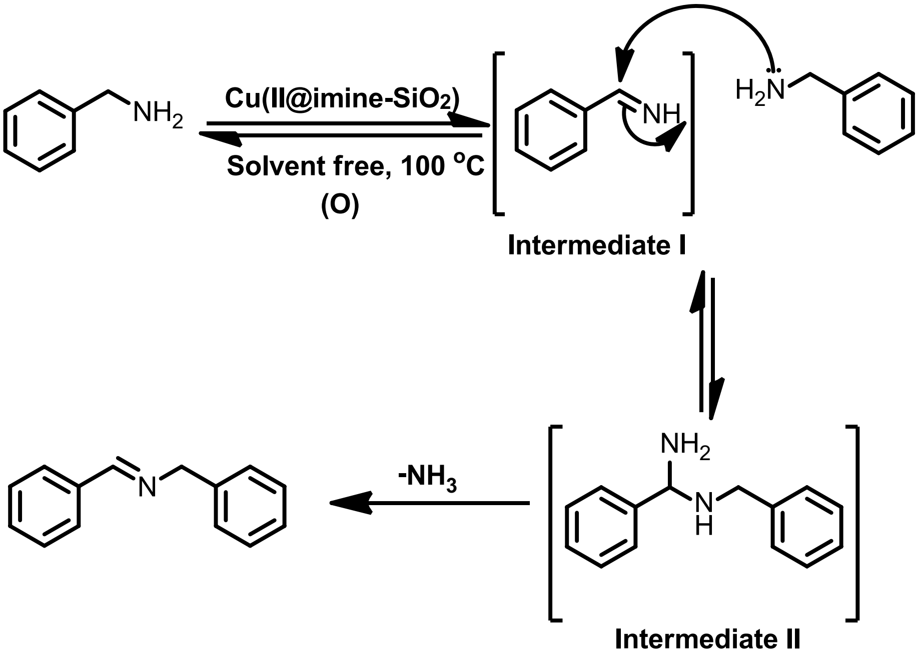

(Table 3, entry 1). So, we have performed a model oxidation reaction by using different quantity (10, 20, 40, 50 and 100 mg) of Cu(II)@imine–SiO_2 as a catalyst under solvent free conditions at 100 °C and the results are shown in Table 3.

It was evident from the Table 3, we assumed that while increasing the catalyst amount from 10 to 50 mg, the yield of the product also gradually increases up to 50 mg (Table 3, entries 2–6). When we carried out a reaction above 50 mg, there is no change in the reaction rate as well as product yield (Table 3, entry 7). Then, we optimized the suitable temperature for this reaction, for this purpose we made a reaction at different temperature such as RT, 50, 80, 100 and 120 °C and observed that 100 °C was found to be optimum temperature for this reaction in terms product yield as well as reaction time (Table 3).

From this optimization results, we concluded that 50 mg of Cu(II)@imine–SiO_2, 100 °C under solvent free condition is most suitable for this reaction. Under this optimized reaction conditions, we have synthesized a variety of imines from the differently substituted benzylamines and their results are summarized in Table 4. Both electron donating as well as electron withdrawing substituent present in the any one of the position of benzylamines were reacted well and provided the corresponding products in good to excellent yields.

Next, we have proposed a possible mechanism for this reaction in Scheme 3. The aerobic oxidation of benzylamine into dibenzylimine usually follows two steps. In the first step, an imine intermediate **I** (PhCH = NH) was formed through the oxidative dehydrogenation of benzylamine. In the next step, the unstable imine intermediate reacts instantly with another molecule of benzylamine to form an aminal intermediate **II** and the final dibenzylimine was formed with the subsequent loss of ammonia [22, 23].

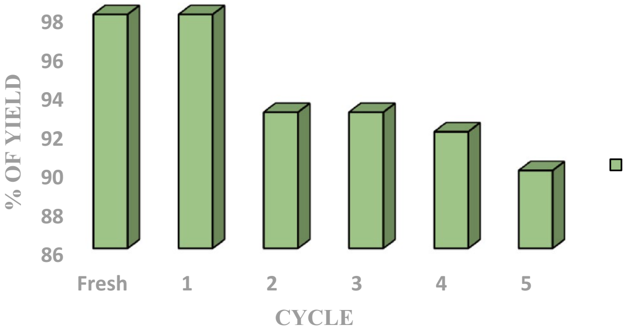

Fig. 6 Reusability of the Cu(II)@imine–SiO_2

Finally, we have checked the reusability of the catalyst [Cu(II)@imine–SiO_2], after completion of the reaction the catalyst was recovered, washed twice with hot ethanol and dried. Then the recovered catalyst was recycled and reused for five consecutive runs without any appreciable change in its catalytic activity (Fig. 6).

The catalytic efficiency of the synthesized material Cu(II)@imine–SiO_2 was compared with the other earlier reported catalysts and the results are presented in the Table 5. From this comparison Table 5, we suggested that the efficiency of the Cu(II)@imine–SiO_2 catalyst is comparable or better than the reported catalysts.

Table 5 Comparison of efficiency of the prepared catalysts with some reported catalysts

Entry	Catalyst	Conditions	Time (h)	Yield (%)	References
1	CuCl (0.5%)	Neat, 100 °C	18	88[b]	[24]
2	Copper-catalyzed (0.5 mol%)	Neat conditions at 90 °C	20	99[b]	[25]
3	Cu^{2+}/4A	120 °C, 14 h Neat conditions	14	97[b]	[26]
4	$Fe(NO_3)_3$/TEMPO (5/5 mol%)	Additive, air, toluene 80 °C	24	97[a]	[27]
5	H_2O_2 (30% in water; 1 mmol)	100 °C	16	69[b]	[28]
6	Cu(II)@imine–SiO_2 (50 mg, 0.257% Cu)	Solvent free at 100 °C, 2 h	2	98[b]	This work

[a] Determined by GC–MS

[b] Isolated products

4 Conclusion

In conclusion, we have successfully prepared the 2-thiophenecarboxaldehyde based copper(II) Schiff base complex immobilized silica material. The synthesized catalyst was completely characterized by FT-IR, UV–DRS, XRD, SEM, EDX, ICP-AES and BET analysis. The synthesized catalyst exhibited the excellent catalytic activity towards the oxidative coupling reaction of benzylamines to the corresponding imines. Excellent yields in shorter reaction time, nominal catalyst loading, use of atmospheric air as an environmentally-friendly oxidant and mild reaction conditions are added advantages of the present methodology. In addition to that, the catalyst was effectively reused for five times without significant loss of its catalytic activity.

Funding The funding was provided by Periyar University

References

1. J.S.M. Samec, A.H. Ell, J.E. Backvall, J. Chem. Eur. **11**, 2327 (2005)
2. J. P. Adams, J. Chem. Soc. Perkin Trans. **1**, 125 (2000)
3. S. Kobayashi, Y. Mori, J.S. Fossey, M.M. Salter, Chem. Rev. **111**, 2626 (2011)
4. R. Neumann, M. Levin, J. Org. Chem. **56**, 5707 (1991)
5. A.H. Ell, J.S.M. Samec, C. Brasse, J.E. Backvall, Chem. Commun. **10**, 1144 (2002)
6. B. Gnanaprakasam, J. Zhang, D. Milstein, Angew. Chem. Int. Ed. **122**, 1510 (2010)
7. S. Yamazaki, Y. Yamazaki, Bull. Chem. Soc. Jpn. **63**, 301 (1990)
8. M.N. Pahalagedara, L.R. Pahalagedara, D. Kriz, S.Y. Chena, F. Beaulieua, W. Thalgaspitiyaa, S.L. Suiba, Appl. Catal. B **188**, 227 (2016)
9. M. Kaur, S. Sharma, S.P.M. Bedi, Chin. J. Catal. **36**, 520 (2015)
10. S. Yajima, T. Nakajima, M. Higashi, K. Kimura, Chem. Commun. **46**, 1914 (2010)
11. R. Qu, Y. Zhang, W. Qu, C. Sun, J. Chen, Y. Ping, H. Chen, Y. Niu, Chem. Eng. J. **219**, 51 (2013)
12. A. Magro, L. Crociani, C. Prinzivalli, P.A. Vigato, P.L. Zanonato, S. Tamburini. Inorg. Chim. Acta **410**, 29 (2014)
13. Q. Wang, W. Gao, Y. Liu, J. Yuan, Z. Xu, Y. Li, M. Schroder, Chem. Eng. J. **8**, 187 (2014)
14. R. Antony, S.T.D. Manickam, K. Karuppasamy, P.V. Chandrasekarc, S. Balakumar, RSC Adv. **4**, 42816 (2014)
15. P. Sharma, A. Lazar, A. Singh, Appl. Catal. A **439**, 101 (2012)
16. T.R. Arun, N. Raman, Spectrochim. Acta Part A **127**, 292 (2014)
17. M.R. Prasad, G. Kamalakar, S.J. Kulkarni, K.V. Raghavan, J. Mol. Catal. A **186**, 109 (2002)
18. W.J. Zhou, B. Albela, P. Perriat, M.Y. He, L. Bonneviot, Langmuir **26**, 13493 (2010)
19. N. An, W. Zhang, X. Yuan, B. Pan, G. Liu, M. Jia, W. Yan, W. Zhang, Chem. Eng. J. **215**, 1 (2013)
20. J. Wang, J. Sun, Y. Li, F. Wang, Luminescence **29**, 188 (2014)
21. K.S.W. Sing, D.H. Everett, R.A.W. Haul, L. Moscou, R.A. Pierotti, J. Rouquerol, T. Siemieniewska, Pure Appl. Chem. **57**, 603 (1985)
22. P. Sudarsanam, A. Rangaswamy B.M. Reddy, RSC Adv. **4**, 46378 (2014)
23. K.N. Tayade, M. Mishra, J. Mol. Catal. A **382**, 114 (2014)
24. R.D. Patil, S. Adimurthy, Adv. Synth. Catal. **353**, 1695 (2011)
25. R.D. Patil, S. Adimurthy, RSC Adv. **2**, 5119 (2012)
26. A. Magyar, Z. Hell, Monatsh. Chem. **147**, 1583 (2016)
27. E. Zhang, H. Tian, S. Xu, X. Yu, Q. Xu, Org. Lett. **15**, 2704 (2013)
28. X.F. Wu, A. Petrosyan, T.V. Ghochikyan, A.S. Saghyan, P. Langer. Tetrahedron Lett. **54**, 3158 (2013)